EFDA–JET–PR(08)24

P. Mantica, D. Strintzi, T. Tala, C. Giroud, T. Johnson, H. Leggate, E. Lerche, T. Loarer, A.G. Peeters, A. Salmi, S. Sharapov, D. Van Eester, P.C. de Vries, L.Zabeo, K.-D.Zastrow and JET EFDA contributors

Experimental Study of the Ion Critical Gradient Length and Stiffness Level and the Impact of Rotation in the JET Tokamak

Experimental Study of the Ion Critical Gradient Length and Stiffness Level and the Impact of Rotation in the JET Tokamak

P. Mantica[1], D. Strintzi[2], T. Tala[3], C. Giroud[4], T. Johnson[5], H. Leggate[4], E. Lerche[6], T. Loarer[7], A.G. Peeters[8], A. Salmi[9], S. Sharapov[4], D.Van Eester[6], P.C. de Vries[4], L. Zabeo[4], K.-D.Zastrow and JET EFDA contributors*

JET-EFDA, Culham Science Centre, OX14 3DB, Abingdon, UK

[1]Istituto di Fisica del Plasma 'P.Caldirola', Associazione Euratom-ENEA-CNR, Milano, Italy
[2]National Technical University of Athens, Association Euratom - Hellenic Republic, GR-15773 Athens, Greece
[3]Association EURATOM-Tekes, VTT, P.O. Box 1000, FIN-02044 VTT, Finland
[4]EURATOM-UKAEA Fusion Association, Culham Science Centre, OX14 3DB, Abingdon, OXON, UK
[5]Association EURATOM - VR, Fusion Plasma Physics, EES, KTH, Stockholm, Sweden
[6] LPP-ERM/KMS, Association Euratom-Belgian State, TEC, B-1000 Brussels, Belgium
[7]CEA Cadarache, Association EURATOM-CEA, 13108, St Paul-Lez-Durance, France
[8]Centre for Fusion Space and Astrophysics, University of Warwick, Coventry 7AL, UK
[9]Association EURATOM-Tekes, Helsinki University of Technology, P.O. Box 2200, FIN-02150 TKK, Finland
** See annex of M.L. Watkins et al, "Overview of JET Results ",*
(Proc. 21 st IAEA Fusion Energy Conference, Chengdu, China (2006)).

Preprint of Paper to be submitted for publication in
Physical Review Letters

ABSTRACT

Experiments have been carried out in the JET tokamak in order to determine the critical ion temperature inverse gradient length ($R/L_{Ti} = R|\nabla T_i|/T_i$) for the onset of Ion Temperature Gradient modes and the stiffness of T_i profiles with respect to deviations from the critical value. Threshold and stiffness have been identified and compared with linear and non-linear predictions of the gyro-kinetic code GS2. Comparison of plasmas with different values of toroidal rotation indicates a significant increase in R/L_{Ti} in rotating plasmas. Various experimental observations allow to conclude that such increase is mainly due to a decrease of the stiffness level with increasing rotation, rather than to a mere up-shift of the critical value, as commonly predicted by theory. This finding has implications on the interpretation of present day experimental results on the effect of rotation on confinement as well as on extrapolations to future machines.

1. INTRODUCTION

The anomalous character of ion heat transport in tokamaks, 1-2 orders of magnitude higher than collisional transport, is a long dated experimental observation. Recent studies are reported e.g. in [1-3]. A comprehensive theoretical description of turbulent ion heat transport as driven by Ion Temperature Gradients (ITG) modes has been developed and applied to physics based predictions of confinement in present and future devices [4-7]. ITGs feature a threshold in the inverse ion temperature gradient length ($R/L_{Ti} = R|\nabla T_i|/T_i$, with R the tokamak major radius) above which the†ion heat flux (q_i) increases strongly with R/L_{Ti}. This property leads to stiffness of T_i profiles with respect to changes in heating profiles. The level of stiffness characterizes how strongly T_i profiles are tied to the threshold. Experimental observations in several devices of the correlation between edge and core T_i values [1,8-10] support this theoretical picture. However, no dedicated experimental studies have yet been performed of the existence and value of a critical R/L_{Ti}, its dependences on plasma parameters and up-shifts due to rotational shear or non-linear effects, as predicted by theory. Also, no experimental determination of the response of q_i to an increase in R/L_{Ti}, yielding the stiffness level, has yet been made, although recent T_i modulation experiments in JET [11] have provided the first measurements of the ion stiffness level by determining the local slope of the q_i vs R/L_{Ti} curve. The issue is of high relevance for the operation of future generation devices, because the core T_i and fusion power achievable for a given T_i pedestal depend crucially on threshold and stiffness.

Ion heat transport experiments are not easily performed as they require both a good ion diagnostic and an efficient and flexible ion heating scheme for shaping the ion power deposition profile. The JET tokamak (R=2.96m, a=1m) is equipped with a high quality active Charge Exchange Spectroscopy (CX) diagnostics for T_i and toroidal rotation (ω_t) measurements and a multi-frequency Ion Cyclotron Resonance Heating (ICRH) system for flexible and fairly localized ion heating either using (H)-D or (^{3}He)-D minority schemes. These tools, together with JET s large size and low normalized ion gyro-radius, make it an ideal device to perform on ions studies of threshold and stiffness as earlier performed on electrons [12-14]. This letter describes first experiments in JET determining the ITG threshold and

stiffness in low rotation plasmas, comparison with theory, and an experimental evaluation of the impact of rotation.

Experimentally the identification of the ITG threshold and stiffness requires a scan of the core q_i at constant edge q_i, to keep edge properties constant, whilst maintaining reasonably unchanged other plasma parameters such as density, safety factor profile, T_e/T_i, Z_{eff}, rotation. Both electron and ion heat fluxes are predicted by theory to follow a gyro-Bohm scaling, at least for low values of the normalized gyro-radius, so that q_i can be written in a general way as [15] where q_i^{res} is the residual flux, including the neoclassical flux and possible contributions to ion transport not driven by ITG, n_i the ion density, q the safety factor, B the magnetic field, e the electron charge, $\rho_i = (m_i T_i)^{1/2}/eB$, m_i the ion mass and H the Heaviside step function. Therefore, from the curve of the gyro-Bohm normalized flux q_i^{norm} vs R/L_{Ti}, the threshold R/L_{Ticrit} can be identified as the intercept at neoclassical flux and the stiffness level χ_s can be inferred from the slope. This implies a normalization of q_i over a factor $n_i q^{1.5} T_i^{5/2}/R^2B^2$. In the following n_e was taken as an estimator for n_i, since the plasmas have similar impurity content (Z_{eff}~2-2.5). The normalization is not important for the threshold identification but is essential to extract the correct intrinsic stiffness level χ_s. Far from threshold q_i is theoretically foreseen to be linear with R/L_{Ti} [16]. In the range of q_i covered by the experiments, not too far from threshold, the experimental uncertainties do not allow to distinguish between linear and quadratic dependence. To allow comparison with previous work on electron stiffness, following the semi-empirical critical gradient model (CGM) described in [17], in the empirical modelling described below $f(R/L_{Ti})$ was assumed to be linear, so that q_i is quadratic in R/L_{Ti}.

The experiment was performed in JET L-mode plasmas with B_T=3.36T, I_p=1.8MA, q_{95}~6 (to minimize core sawtooth activity), n_{e0}~3-4 $10^{19}m^{-3}$, $0.9<T_e/T_i$~1.2. The need to reach low values of q_i^{norm} to identify the threshold requires to minimize the centrally deposited power from Neutral Beam Injection (NBI). Therefore the experiment was done in low rotating plasmas, retaining only the CX diagnostic NBI beam (1.5 MW). Most of heating was then provided by ICRH (3-6 MW), using the multi-frequency capability to vary the ion power distribution between on- and off-axis (ρ_{tor}~0.6, where ρ_{tor} is the square root of the normalized toroidal magnetic flux). ICRH was applied in a (H)-D scheme (51 MHz on-axis, 42 MHz off-axis) with H concentration ~8% and 30-60% of the ICRH core power delivered to thermal ions, and in a (^{3}He)-D scheme (33 MHz on-axis, 29 MHz off-axis) with ^{3}He concentration ~7% and 50-80% of the ICRH core power delivered to thermal ions. Values of R/L_{Ti} were averaged in time over the stationary intervals and calculated with respect to the flux surface minor radius $\rho=(R_{out}-R_{in})/2$, where R_{out} and R_{in} are the outer and inner boundaries of the flux surface on the magnetic axis plane. The values of q_i have been calculated using the SELFO [18] code for ICRH and the PENCIL [19] code for the NBI power. The resulting q_i^{norm} vs R/L_{Ti} plot is shown in Fig.1 (red circles). Error bars are not plotted for clarity's sake, they are typically $\Delta R/L_{Ti}$~±0.3-0.6 and Δq_i^{norm} ~±0.1 MW. The points at neoclassical level were obtained by slowly modulating the NBI CX beam to measure just after switch-on the T_i profile corresponding to zero NBI power. The gyro-Bohm normalization has been applied to q_i in two ways, to meet the inclinations of both experimentalists and

theoreticians. The left scale of Fig.1 indicates the total power in MW within ρ_{tor}=0.33 and is normalized over $n_e T_i^{5/2}/R^2B^2$ by rescaling the power to reference values T_i=1.85 keV, n_e=3 10^{19} m^{-3}, B_T=3.36T. The $q^{1.5}$ dependence was not included in the normalization because the local q has small variations across the dataset (q~1.2-1.5) and with large relative experimental uncertainties. The right scale indicates the values of q_i at ρ_{tor}=0.33 in gyro-Bohm units, i.e. q_i^{gB} [gB-units]= q_i [MW/m^2] / [$(\rho_i/R)^2 v_{ith} n_i T_i$], where $v_{ith}=\sqrt{T_i/m_i}$. The threshold is well identified experimentally in Fig.1 as the intercept at neoclassical heat flux. The ion stiffness appears to be high, as the available excursion of q_i^{norm} by more than one order of magnitude does not lead to a significant change in R/L_{Ti}.

Blue triangles and black squares in Fig.1 indicate high NBI power discharges with similar parameters but different levels of power and torque. Due to the gyro-Bohm normalization, they cover a similar range of q_i^{norm} as the low rotation shots. However, they show a significant increase of R/L_{Ti} with increasing rotation.

In the high rotation discharges the threshold is not directly identified by low q_i^{norm} points, therefore the key question is whether the increase in R/L_{Ti} is due to an effect of rotational shearing rate (ω_{ExB}) on the threshold only, in accordance with theory predictions (i.e. keeping the same slope for all curves), or also on the stiffness level, as the data in Fig.1 suggest. In the first case, one would need a shift in threshold $\Delta R/L_{Ti}$~4, which is much larger than the value $\Delta R/L_{Ti}$~1 predicted by the so-called†"Waltz rule"[20]: $\gamma=\gamma_{lin}-\alpha_E\ \omega_{ExB}$ with α_E~0.6 [21]. Such a high shift in threshold is very difficult to justify especially given the high stiffness measured in the low rotation shots. Assuming, instead, the validity of the Waltz rule for the shift in threshold, an upper limit for the change in the intrinsic stiffness coefficient χ_s has been estimated by fitting the data using the CGM [17]. The dotted lines in Fig.1 indicate a change of χ_s from 7 to 0.5 with increasing rotation, leading to a factor 3 increase in R/L_{Ti} at similar values of the normalized heat flux. We attribute this variation to rotation because both its central value and its gradient change by a factor 6 over the dataset, whilst other parameters have only minor variations. Some variation is present in the ratio $R/L_{Te}/R/L_{Ti}$, which is ~1 in high rotation shots, and varies between 1.2 and 1.9 with increasing heat flux in low rotation shots. This is inherent in the fact that electrons are found less stiff than ions at low rotation, and the unavoidable fraction of ICRH electron power is sufficient to induce an increase of R/L_{Te} whilst R/L_{Ti} is blocked at the threshold by the high ion stiffness. On the other hand, since the ion heat flux driven by R/L_{Te} is generally negligibile [11], we do not believe that such variation may affect our conclusions.

Since a more significant effect of rotation on stiffness than on threshold is a new observation, apparently not predicted by present theories, additional experimental evidence has been sought for confirmation. First of all, T_i modulation experiments in (^{3}He)-D provide a direct measurement of the local slope in the q^{norm} vs R/L_{Ti} diagram. First experiments in rotating plasmas [11], indicating moderate stiffness levels, have been repeated both in low and high rotation plasmas to seek an independent confirmation of the factor 10 variation of stiffness level observed in the steady-steady plot in Fig.1. 35 square wave power modulation cycles at $\omega/2\pi$=6.25 Hz were performed, with 3 MW of ICRH power with on-axis deposition and duty-cycle 70%, to provide both 1st and 2nd harmonic components of the

modulation. Fig.2 shows the amplitude (A) and phase (φ) profiles of the T_i perturbation at 6.25 and 12.5 Hz for two shots belonging respectively to the red circle and black square sets in Fig.1. It is immediately evident from the slopes of A and φ in Fig.2 that the incremental diffusivity $\chi_i^{inc}=-\partial q_i/n_i\partial\nabla T_i$ is much higher in the low rotation shot. A simple analysis calculating χ_i^{inc} from of the φ slopes ($\chi_i^{inc}=3/4\omega/\varphi'^2$, [9]) yields $\chi_i^{inc}=12$ m^2/s at low rotation and 2.6 m^2/s at high rotation. The ratio with the power balance heat diffusivity ($\chi_i^{PB}=-q_i/n_i\nabla T_i$) is 5 and 1.9 respectively. Normalizing by $T_i^{3/2}$ further enhances the difference, because high rotation shots are also hotter. The slopes derived from this analysis are indicated in Fig.1 by the two solid segments.

A more refined determination of the intrinsic stiffness coefficient χ_s was obtained with a time dependent transport simulation with the ASTRA code [22] using the CGM model [17]. The resulting A and φ profiles are also plotted in Fig.2. The width of the ion deposition and the ion coupled power have been taken from SELFO, as well as the indication of the fast ion slowing down time that determines the φ absolute values. The contribution of the T_e modulation to the T_i modulation due to collisional coupling is found about 10% at 6.25 Hz and insignificant at 12.5 Hz. The modulation data (and the steady-state, not shown) can overall be satisfactorily fitted using $R/L_{Ti,crit}=3.5$, $\chi_s=3$ at low rotation and $R/L_{Ti,crit}=4$, $\chi_s=0.3$ at high rotation. We conclude that the T_i modulation data directly confirm the factor 10 decrease in stiffness level seen in Fig.1 with increasing rotation. The small discrepancy in χ_s values with respect to those indicated in Fig.1 may depend on the fact that the modulation extracts χ_s from a single shot but fitting the spatial profiles of A and φ with an effective stiffness scaling with radius as in Eq.(1), whilst the steady-state analysis of Fig.1 is local at $\rho_{tor}=0.33$, but the fit is then made on a set of shots. In addition, one must be aware that the uppermost low rotation shots in Fig.1 have $T_e/T_i=1.1$-1.2, which according to theory implies a downshift in threshold from 3.6 to 3.2, yielding some overestimate of χ_s.

Secondly, the comparison of co- and counter-NBI plasmas with otherwise identical parameters (by reversing B_T and I_p in a dedicated campaign) shows that counter-NBI plasmas with very flat rotation profiles exhibit much lower R/L_{Ti} than co-NBI plasmas with peaked rotation. The comparison of ω_t and T_i profiles for a pair of co- and counter-NBI discharges is shown in Fig.3. The flatter and lower toroidal rotation in the counter-NBI case is ascribed to off-axis torque deposition, also shown in Fig.3a [23]. The non-normalized q_i is similar as shown in Fig.3b (only 25% less ion heat flux in the counter-NBI case, which does not in itself justify the dramatic T_i decrease). Due to the lower T_i, the counter-NBI shot has a higher normalized heat flux, nevertheless a dramatic reduction of R/L_{Ti} from 5.2 to 3.5 is observed (Fig.3b). In a q_i^{norm} vs R/L_{Ti} type of plot, the analysis of these pairs of co- and counter-NBI shots yields Fig.4, which makes use of various times during the density ramp-up leading to rotation decreasing in the counter-NBI case, and remaining peaked in the co-NBI case. The final states of co- and counter NBI shots (as shown in Fig.3) indicate again a very important difference in stiffness level, whilst being compatible with a similar threshold. Lines in Fig.4 are indicative of the CGM model stiffness levels compatible with the data.

Thirdly, experiments in which NBI power is substituted with ICRH (H)-D power at constant total power have also been performed in JET H-mode plasmas [24] and the resulting q_i^{norm} vs R/L_{Ti} plot is shown in Fig.5, confirming the high level of stiffness in low rotation plasmas. Unlike in Fig.1, due to the constraint of preserving total power, high rotation NBI dominant plasmas did not achieve as high range of variation of q_i^{norm} as low rotation ICRH dominant plasmas due to the broader power deposition of NBI compared with ICRH. Therefore whilst the small shift in threshold due to the combined effect of increased rotational shear and lower T_e/T_i is visible, nothing can be assessed from this type of experiments on the decrease of the stiffness level in the high rotation case, preventing a conclusive assessment of the role of rotation on core transport.

Overall, we conclude that the available experimental evidence points consistently to a significant effect of rotation on ion stiffness in addition to a smaller effect on threshold.

The GS2 gyrokinetic code [25] has been used linearly and non-linearly to compare theory predictions with experimental results. The code does not include background ExB shear and thus cannot address effects of sheared plasma rotation and can only be compared to the low rotation data. Very good agreement is found between the linear GS2 threshold (indicated by the arrow in Fig.1) and the value found in the experiment. The GS2 linear threshold has also been cross-checked with the linear threshold by the GENE [26], GKW [27] and GYRO [28] gyro-kinetic codes with very close match amongst the different codes. Minor variations were found in the linear threshold across the discharges in Fig.1, indicating that the increase in R/L_{Ti} in high rotation plasmas cannot be ascribed to a change in linear threshold associated to minor variations of plasma parameters. Parameter scans indicate that in these plasmas the linear threshold is mainly sensitive to T_e/T_i and q, whilst R/L_n and magnetic shear play a minor role. The non-linear GS2 predictions are drawn in Fig.1 as a short-dashed red and long-dashed violet lines, with and without ion-electron collisions respectively. Adding also ion-ion collisions does not change the curve. The collisionless runs yield a slope close to the experimental one, but an up-shifted non-linear threshold R/L_{Ti}~4.8, with a significant Dimits shift. The experimental data however do not support such shift and remain close to the linear threshold. The collisional runs, which have to be regarded as more realistic, have a similar slope far from threshold, whilst approaching the threshold they deviate from the linear trend indicating a finite transport below the up-shifted threshold. In this case the non-linear threshold coincides with the linear one and the curve yields no prediction of a non-linear up-shift. However, the stiffness level in the q_i^{norm} range of the experiments turns out then to be significantly lower than in experiment. We conclude that non-linear GS2 simulations are not found in agreement with experiments. The new result of a decrease in stiffness level with increasing rotation cannot be addressed by GS2 and requires more complex numerical tools. To our knowledge, no prediction in this direction exists so far and deeper theoretical investigation is required.

The implication of these findings is that rotation effects on stiffness cannot be ignored in addition to effects on threshold when interpreting experiments in present day machines aimed at identifying the role of rotation on confinement, such as comparison of balanced vs unbalanced NBI [29,30], effects of varying B_T ripple [31], influence of resonant magnetic field perturbations [32]. Such results

require careful, physics based extrapolation to future devices. In fact, depending on how high above threshold in the normalized plot ITER or DEMO will operate (see their position in Fig.1 based on GLF23 simulations), the larger effect of rotation on stiffness may or may not dominate over the smaller effect on threshold. In any case, blind extrapolations of the size of the effect of rotation on core confinement from present devices without knowing in which point of the q_i^{norm} vs R/L_{Ti} diagram the experiment is carried out and in which point ITER/DEMO will operate are not legitimate.

ACKNOWLEDGEMENTS

We are grateful to C.Angioni, V.Naulin and F.Ryter for stimulating discussions. We thank V.Parail and G.V. Pereverzev for providing ITER and DEMO simulations using GLF23. This work, supported by the European Communities under the contract of Association EURATOM/ ENEA-CNR, was carried out within the framework of EFDA. The views and opinions expressed herein do not necessarily reflect those of the European Commission.

REFERENCES

[1] A.G.Peeters *et al.*, Nucl. Fusion **42,** 1376 (2002).
[2] C.C.Petty *et al.*, Phys. Plasmas **9**, 128 (2002).
[3]R.C.Wolf *et al.*, Plasma Phys. Controlled Fusion **45,** 1757 (2003).
[4] N.Mattor *et al.*, Phys. Fluids **31**, 1180 (1988).
[5] F.Romanelli et al., Phys. Fluids B **1**, 1018 (1989).
[6] J.W.Connor and H.R.Wilson, Plasma Phys. Controlled Fusion **36,** 719 (1994).
[7] M.Kotschenreuther *et al.*, Phys. Plasmas **2**, 2381 (1995).
[8] G.Tardini *et al.*, Nucl. Fusion **42,** 258 (2002).
[9] P.Mantica and F.Ryter, C. R. Physique **7,** 634 (2006).
[10] D.R.Mikkelsen *et al.*, Nucl. Fusion **43,** 30 (2003).
[11] F.Ryter *et al.*, in *Proceedings of the 22nd Int. Conf. on Fusion Energy, Geneva, 2008* [IAEA, Vienna, 2008], EX/P5-19.
[12] F.Ryter *et al.*, Phys.Rev.Lett. **95**, 085001-1 (2005).
[13] F.Ryter *et al.*, Plasma Phys. Controlled Fusion **48,** B453 (2006).
[14] A.G. Peeters *et al.*,††Phys. Plasmas **12**, 022505 (2005).
[15] X.Garbet *et al.*, Plasma Phys. Controlled Fusion **46,** B557 (2004).
[16] A.M. Dimits *et al.*, Phys. Plasmas **7**, 969 (2000).
[17] X.Garbet *et al.*, Plasma Phys. Controlled Fusion, **46,** 1351 (2004).
[18] J. Hedin *et al.*, Nucl. Fusion **42**, 527 (2002).
[19] C.D. Challis *et al.*, Nucl. Fusion, **29,** †563 (1989).
[20] R.E. Waltz *et al.*, Phys. Plasmas **1**, 2229 (1994). †
[21] J. Kinsey *et al.*, Phys. Plasmas **14,** 102306 (2007).
[22] G.V. Pereverzev *et al.*, Max-Planck Report, IPP 5/98 (2002).

[23] P.De Vries *et al*., Nucl. Fusion **48,** 065006 (2008).
[24] W.Suttrop *et al*., Europhys.Conf.Abstr.A **25,** 989 (2001).
[25] M. Kotschenreuther et al., Comput. Phys. Commun. **88,** 128 **(**1995).
[26] F. Jenko *et al*., Plasma Phys.Controlled Fusion **47**, B195 (2005)
[27] A.G. Peeters *et al.*, Phys. Plasmas **11**, 3748 (2004).
[28] J.Candy, R. E.Waltz, J. Comput. Phys. **186**, 545 (2003).
[29] T.C. Luce, *et al.*, in *Proceedings of the 21st Int. Conf. on Fusion Energy, Chengdu, 2006* [IAEA, Vienna, 2006], PD-3.
[30] H.Urano et al., Nucl. Fusion **48,** 085007 (2008).
[31] G.Saibene *et al*., in *Proc. of 34th EPS Conference, Warsaw, 2007, ECA* (European Physical Society, 2007), Vol.31F, O-4.001.
[32] Y.Liang *et al*., Phys.Rev.Lett, **98,** 265004 (2007).

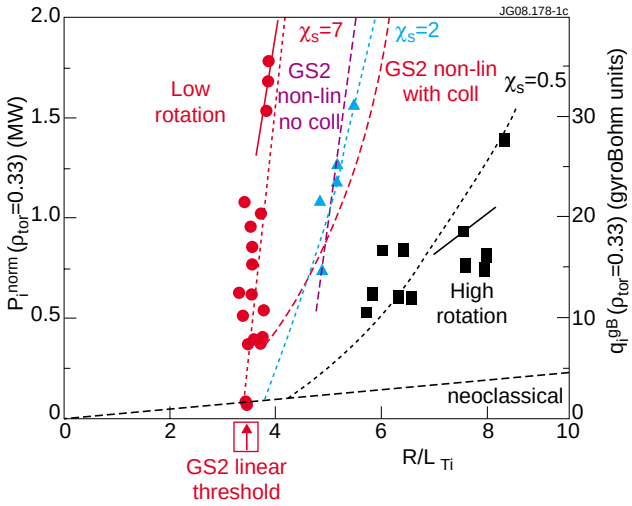

Figure 1: (colors on-line). Normalized q_i at ρ_{tor}=0.33 versus R/L_{Ti} for similar plasmas with different levels of rotation. Dots are experimental data and lines simulations. ●: $1<\omega_t<2\ 10^4$rad/s, ▲: $3<\omega_t<4\ 10^4$rad/s, ■: $5<\omega_t<6\ 10^4$rad/s. The dashed black line is indicative of the neoclassical transport. The 2 segments indicate the local slope deduced from modulation. The 3 dotted lines are simulations using the CGM with different values of χ_s. The dashed thicker red and violet lines are non-linear GS2 simulations with and without collisions, and the red arrow indicates the GS2 linear threshold for the low rotation shots. The ITER and DEMO positions (referring to right Y axis) are marked from simulations using the GLF23 transport model with two assumptions for the pedestal.

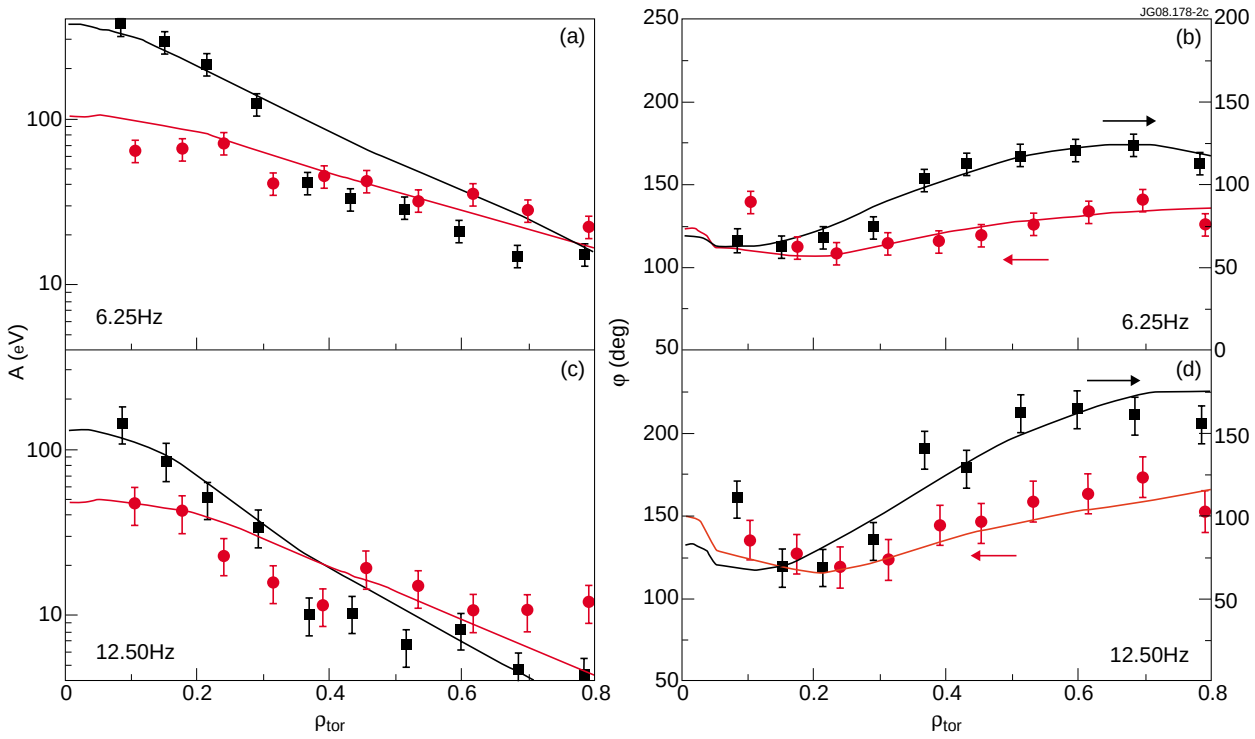

Figure 2: (colors on-line). Dots: experimental, lines: CGM-simulated profiles of A and φ of T_i at 2 modulation frequencies, for a low (Pulse No: 73221, red circles) and a high rotation shot (73224, black squares).

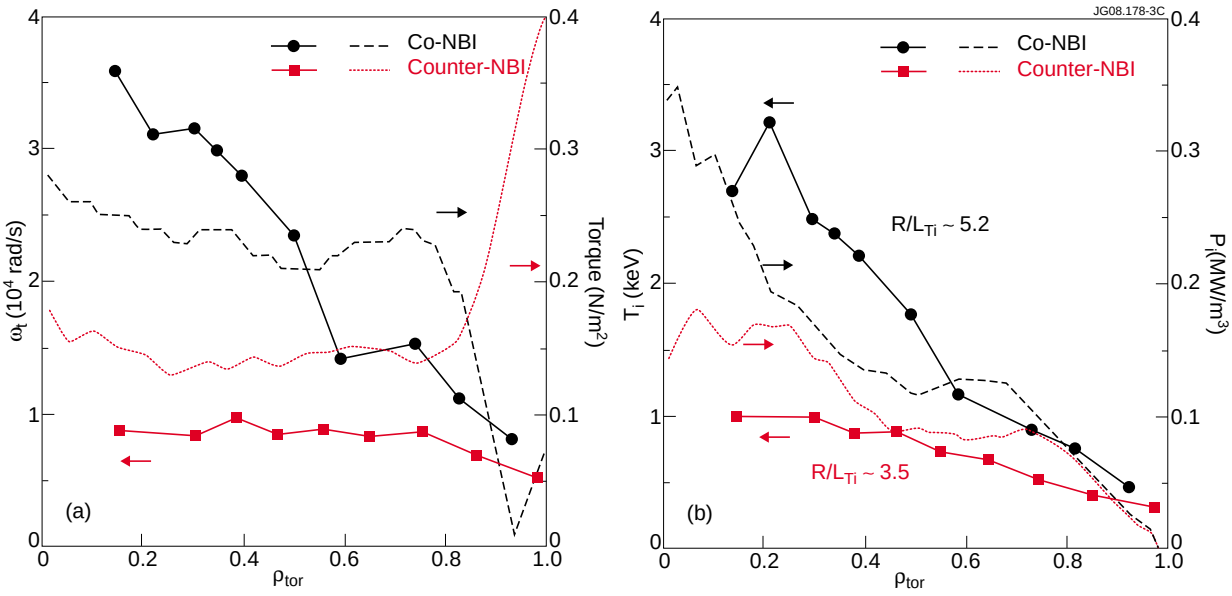

Figure 3: (colors on-line). Comparison of (a) toroidal rotation and torque and (b) T_i and ICRH+NBI ion power density profiles for a pair of similar JET discharges with co- (black circles and dashed lines) and counter-NBI (red

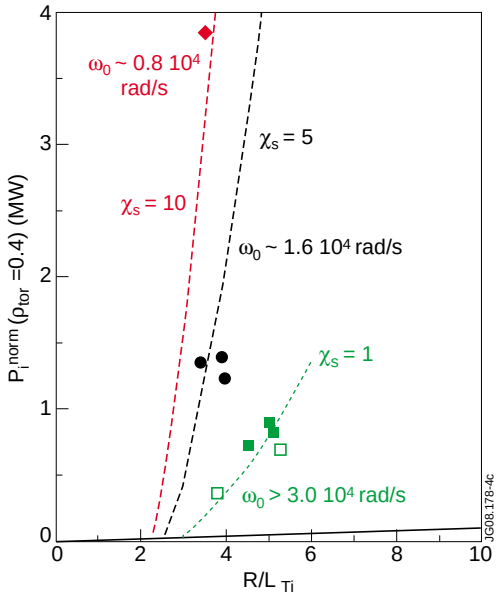

Figure 4: (colors on-line). P_i^{norm} at r_{tor}=0.4 versus R/L_{Ti} for co- (open symbols- Pulse No: 58418) and counter-NBI (full symbols -Pulse No's: 59630, 59637) discharges. Different rotations are marked with different symbols/ colors.

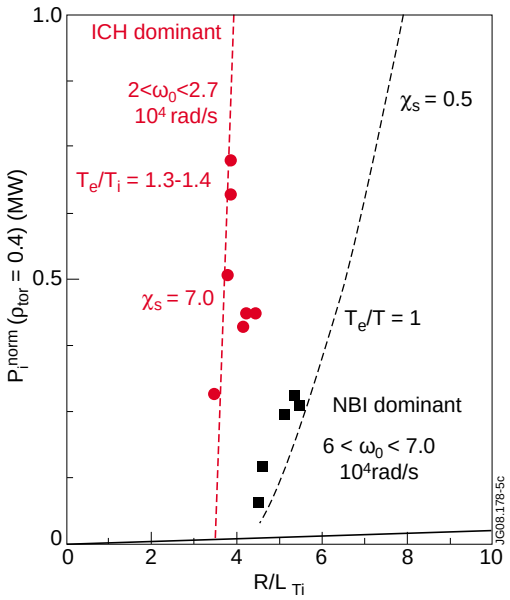

Figure 5: (colors on-line). P_i^{norm} at r_{tor}=0.4 versus R/L_{Ti} in a set of H-mode shots (Pulse No's: 50623-50630; 52092 -52100) where NBI power (black squares) was substituted with ICRH power (red circles). The lines are the CGM model.